

## REACTION OF CRYSTAL STRUCTURES AND REACTION FABRIC

W. R. LAUDER, *Victoria University of Wellington,  
Wellington, New Zealand.*

### ABSTRACT

Reaction fabric is the fabric resulting from the control of the orientation of one mineral by another. It may be produced by exsolution, simultaneous crystallization, parallel growth, and replacement. Such fabrics can be shown on a contoured reaction fabric diagram, which indicates the orientation of one mineral with respect to another that has known orientation. The reaction fabric diagrams of quartz with respect to microcline in micrographic intergrowth, and of albite with respect to labradorite which it replaces, indicate that there is some control of the orientation of quartz by microcline and albite by labradorite.

### INTRODUCTION

When one mineral replaces another some ions from the host mineral often form part of the guest mineral. It is possible, therefore, that the orientation of the crystal structure of the guest will be influenced by the orientation of the structure of the host mineral. Control of the orientation of one mineral by another results in what is termed, in this paper, reaction fabric.

Reaction fabric is most readily recognized in crystals which contain chains, sheets, or bands of  $\text{SiO}_4$  tetrahedra. These structural elements often determine the position of cleavages and the crystallographic form of a mineral, and the relative orientation of the guest and host can be obtained by reference to these properties, *e.g.* in the uralitization of pyroxene bands in the amphibole structure are sometimes parallel to the chains in the pyroxene structure (Fig. 1).

When considering minerals such as quartz and feldspar, however, recourse must be made to the detailed optics of pairs of minerals for the determination of their relative orientation. Although the principal axes of the optical indicatrix do not, in general, coincide with chains, bands, and sheets of ions in such minerals, the relations between structural elements and optical properties are well known, and when using the stereographic net, deviation is easily allowed for. The purpose of this paper is to show how by using the optic properties of minerals the reaction fabric can be determined.

### CONSTRUCTION OF THE REACTION FABRIC DIAGRAM

Hornblende granophyres from Pepin Island, Nelson, New Zealand, contain about thirty per cent of a micrographic intergrowth of quartz and microcline. Using the universal stage, the following procedure has

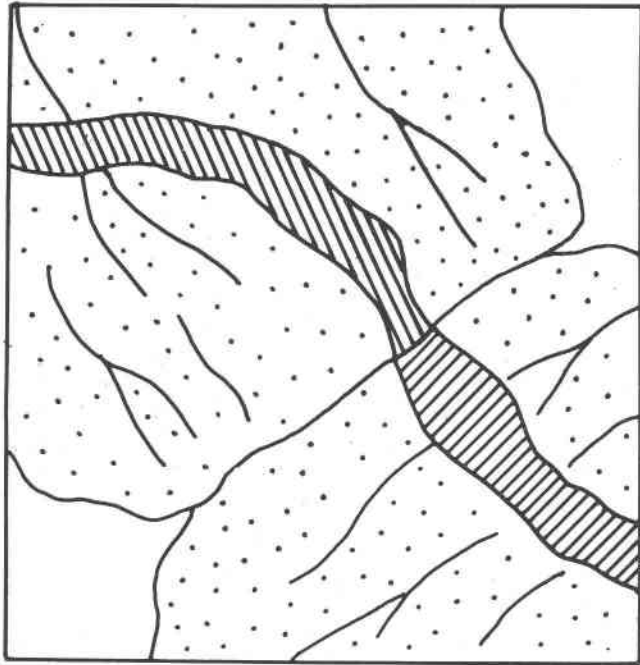


FIG. 1. A uralite vein (lined) crossing two pyroxene crystals (stippled). The fibres of uralite are parallel to the cleavage in the pyroxene.

been used to obtain the equal area plot of the reaction fabric of the  $c$  axis of quartz ( $E_q$ ) with respect to the  $X$  indicatrix axis for microcline ( $\hat{=} a$ ), here described  $X_m$ , in the intergrowths.

(a) Determine the positions of two of the indicatrix axes for microcline ( $X_m$ ,  $Y_m$ , and  $Z_m$ ) in an intergrowth and plot of a Schmidt net (Fig. 2A).

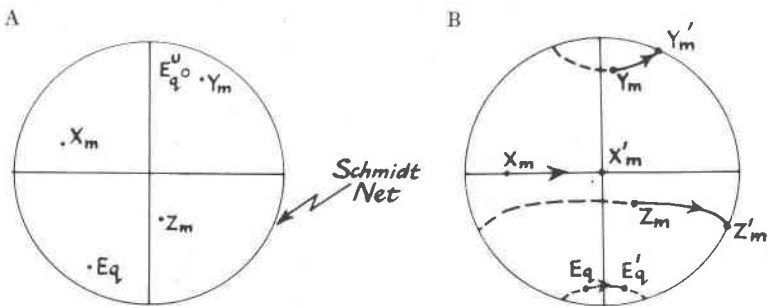


FIG. 2. Plotting of poles on the reaction fabric diagram.  $X_m$ ,  $Y_m$ , and  $Z_m$  are  $X$ ,  $Y$ , and  $Z$  of microcline.  $E$  is  $e$  of quartz.  $E_q^u$  is upper hemisphere. Other points are lower hemisphere.

The position of the third vibration direction is obtained by intersection.

(b) Determine the position of the *c* axis of quartz ( $E_q$ ) in the same intergrowth and plot both upper and lower hemisphere poles on the same sheet as the microcline (Fig. 2A).

(c) Rotate the plot to bring  $X_m$  vertical (Fig. 2B; cf. Phillips 1953, p. 28).  $X'_m$ ,  $Y'_m$ , and  $Z'_m$  are the new positions of  $X_m$ ,  $Y_m$ , and  $Z_m$ , and  $E'_q$  is the new position of  $E_q$ . (Note:  $-X_m \wedge X'_m = Y_m \wedge Y'_m = Z_m \wedge Z'_m =$

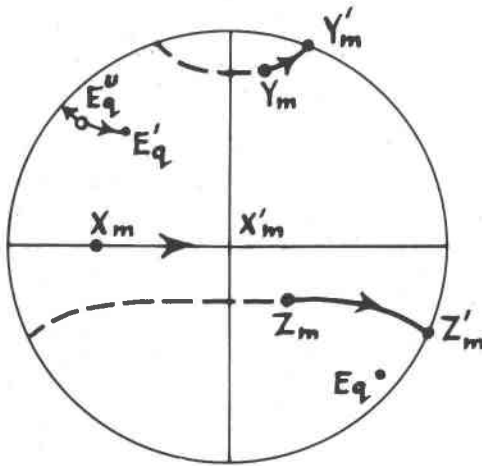


Fig. 3. Plotting of poles on the reaction fabric diagram.  $X_m$ ,  $Y_m$ , and  $Z_m$  are  $X$ ,  $Y$ , and  $Z$  of microcline.  $E_q^u$  is upper hemisphere plot of  $e$  for quartz. Other points are lower hemisphere.

$E_q \wedge E'_q$ ). If during rotation the lower hemisphere pole of quartz ( $E_q$ ) moves on to the upper hemisphere, rotate the upper hemisphere pole  $E_q^u$  (Fig. 3).

(d) Orient the plot so that the  $Y$  vibration direction of microcline coincides with the N-S diameter of the net (Fig. 4A).

$E_q''$  is not a unique position for the  $c$  axis of quartz. There are four positions for a point so derived as shown in Fig. 5. In this diagram the ends of the vibration directions are differentiated to allow the rotations to be reconstructed. This is not so in practice and the four poles are identical. In plotting the reaction fabric diagram all poles have been transferred to the lower left hand quadrant e.g.  $E_q'''$  (Fig. 4B).

(e) The point  $E_q'''$  is now transferred to a new plot (Fig. 4B).

By using the above procedure one hundred  $c$  axes of quartz have been plotted and the contour diagram drawn (Fig. 6). This gives a reaction fabric diagram of quartz with respect to microcline in micrographic intergrowth.

## THE STRUCTURE OF QUARTZ AND MICROCLINE

(a) Quartz (Bragg 1937, p. 83).

Quartz has a three dimensional framework with  $e$  (the slow-ray vibration direction) parallel to the  $c$  crystal axis. There are spiral chains of  $\text{SiO}_4$  tetrahedra with their spiral axes parallel to the  $c$  axis and these chains turn in opposite directions for right- and left-handed quartz.

(b) Microcline (cf. Orthoclase, Bragg 1937, p. 232).

Microcline has a three dimensional framework with the  $X$  vibration direction  $5^\circ$ – $10^\circ$  from the  $a$  crystal axis. Two cleavages (010 and 001)

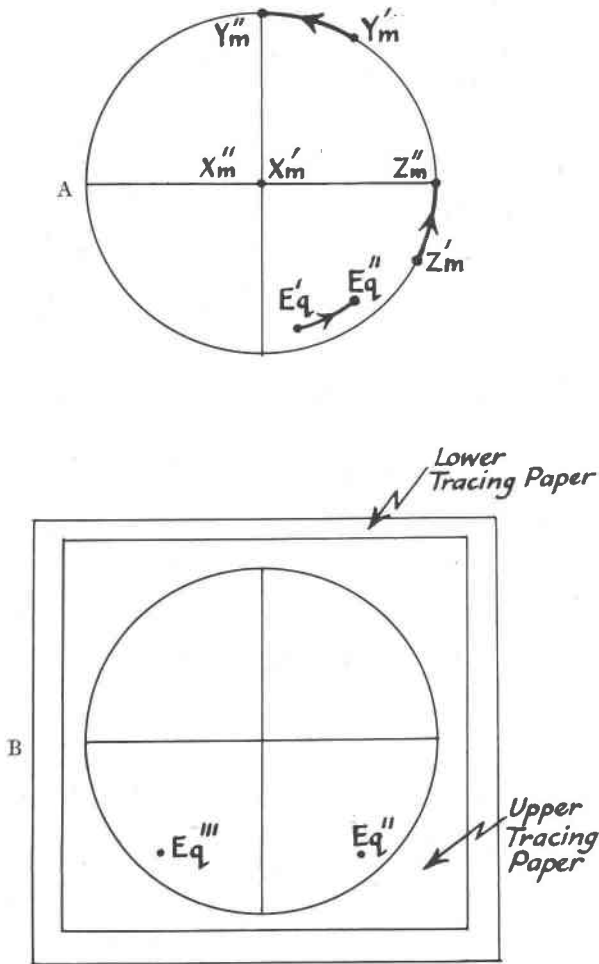


FIG. 4. Plotting of poles on the reaction fabric diagram.  $X_m$ ,  $Y_m$ , and  $Z_m$  are  $X$ ,  $Y$ , and  $Z$  of microcline.  $E_q$  is  $e$  of quartz. Lower hemisphere plot.

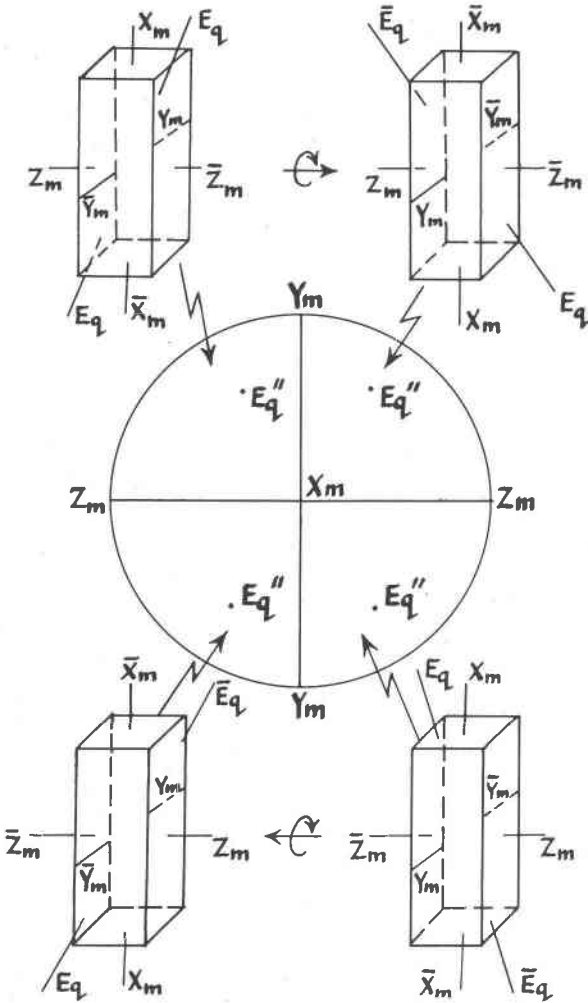


FIG. 5. Four equivalent positions for  $E_q''$ , cf. Fig. 4B. Lower hemisphere plot.  $X_m$ ,  $Y_m$  and  $Z_m$  are  $X$ ,  $Y$ , and  $Z$  of microcline.  $E_q$  is  $e(=c)$  of quartz.

are parallel to  $a$  and these cleavage planes have a high concentration of  $K^+$  ions. Zig-zag chains of  $SiO_4$  tetrahedra run parallel to the  $a$  axis,  $Y \doteq c$  and  $Z \doteq b$ .

INTERPRETATION OF THE REACTION FABRIC DIAGRAM OF QUARTZ WITH RESPECT TO MICROCLINE IN MICROGRAPHIC INTERGROWTH

Figure 6 is a reaction fabric diagram of the  $c$  axes of quartz with respect to microcline in micrographic intergrowth. The poles are dis-

tributed over the whole quadrant. This indicates that there is no single direction in microcline along which the  $c$  axes of quartz are oriented. However, there is a significant concentration of poles on the primitive. In this concentration the  $c$  axes of quartz are oriented more or less perpendicular to the  $a$  axis of microcline ( $a_m$ ) and at about  $45^\circ$  to the  $b$  and  $c$  axes of microcline ( $b_m$  and  $c_m$ ). Thus the spiral chains in the quartz structure are more or less perpendicular to the zig-zag chains in microcline and they intersect the cleavages in microcline at about  $45^\circ$ . By reference to the crystal structure model of microcline, it appears that the  $c$  axes of quartz in this concentration lie in the 001 plane of the felspar.

Micrographic intergrowth probably can be formed either by replacement or by simultaneous crystallization, and in either case a reaction fabric could be produced. In the replacement of microcline ( $\text{KAlSi}_3\text{O}_8$ ) by quartz it is necessary to eliminate the  $\text{K}^+$  ion and substitute silicon

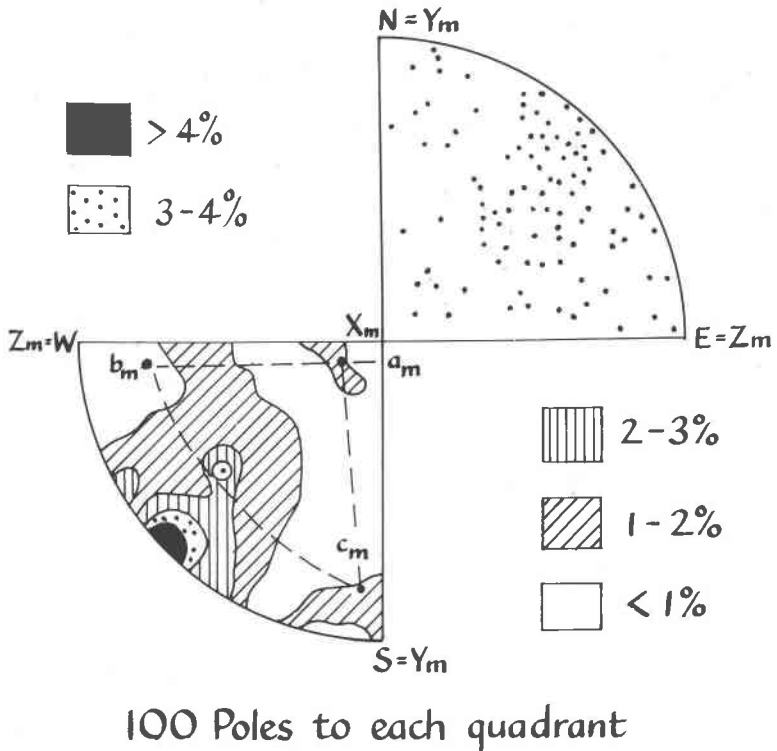


FIG. 6. The reaction fabric diagram of the  $c$  axis of quartz in micrographic intergrowth with microcline when the  $X$  vibration direction of microcline is vertical.  $X_m$ ,  $Y_m$ , and  $Z_m$  are  $X$ ,  $Y$  and  $Z$  for microcline.  $a_m$ ,  $b_m$ , and  $c_m$  are  $a$ ,  $b$  and  $c$  of microcline. Poles plotted and contour diagram. The four per cent contour encloses four per cent of 400 poles, *i.e.*, 16 poles.

for aluminium in the tetrahedra of the framework. The concentration of the  $c$  axes of quartz in the 001 plane of microcline suggests that the concentration of Si-O and Al-O tetrahedra in this plane has allowed the substitution to take place without complete disruption of the silicate framework. It might perhaps be expected that if this were the case the  $c$  axis would grow in this plane and parallel to the 010 cleavage. That this is not so suggests that the bonds in the framework which cross the 010 cleavage plane, although few in number, are Si-O rather than Al-O bonds. This allows the bridging of the cleavage planes without disruption of the silicate framework.

If simultaneous crystallization produced the intergrowths, then it is possible that the quartz nuclei encrusted the 001 plane of the microcline with a concentration of  $c$  axes parallel to 001 and at  $45^\circ$  to 010. However, in vugs and veins quartz crystals tend to grow so that the  $c$  axes are more or less perpendicular to the surface on which they start crystallization. It is unlikely, therefore, that the reaction fabric was produced by growth of quartz crystals on either the 001, or the 010, plane of the microcline.

#### THE REACTION FABRIC DIAGRAM OF THE $a$ AXIS OF ALBITE WITH RESPECT TO LABRADORITE WHICH IT REPLACES

In basalts of Markle Type from Arthur's Seat, Edinburgh (Clark 1956), many of the labradorite phenocrysts are partially replaced by albite. The mineral fabric diagram of the  $a$  axes of albite with respect to the labradorite has been derived in the following way:—

For any one crystal the position of the  $X$ ,  $Y$  and  $Z$  indicatrix directions of albite and labradorite were measured and plotted on a Schmidt net. The position of the  $a$  axis of albite was located in relation to the vibration directions of that mineral. The plot was then rotated so that the  $X$  axis of labradorite ( $X_l$ ) was vertical, the  $Z$  axis ( $Z_l$ ) along the E-W diameter of the net, and the  $Y$  axis ( $Y_l$ ) along the N-S diameter. The position of the  $a$  axis of albite was then transferred, if necessary, to the lower left hand quadrant and plotted on a separate oriented sheet.

#### *The Structure of Albite and Labradorite*

The structures of these minerals are similar to that of orthoclase—a three dimensional framework of Si-O and Al-O tetrahedra with zig-zag chains parallel to the  $a$  crystal axes. The  $c$  axis of the unit cell of labradorite is twice as long as that in the unit cell of albite.

#### *The Interpretation of the Reaction Fabric Diagram of Albite Replacements of Labradorite*

Figure 7 shows a concentration of the poles of the  $a$  axis of albite in the  $a$ - $c$  plane (010) of labradorite with a relatively strong concentration

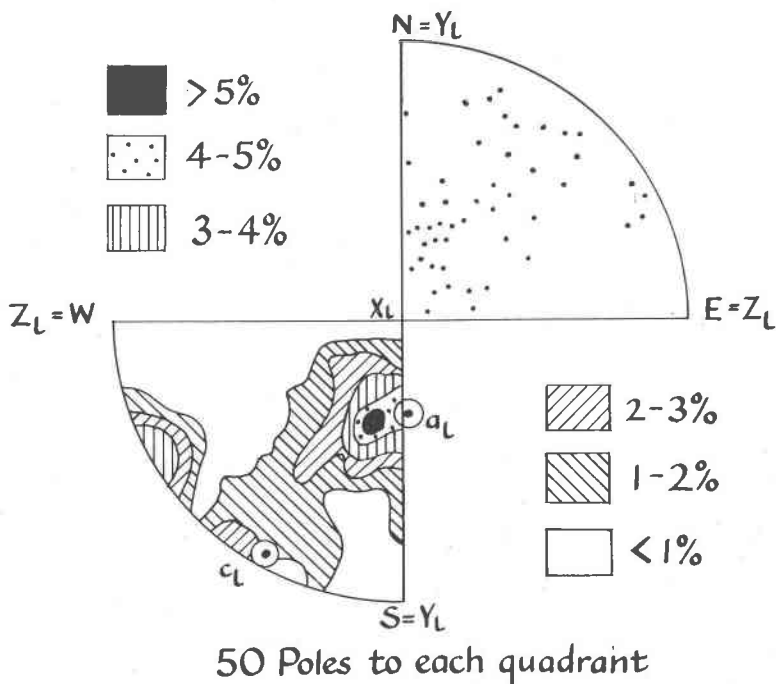


FIG. 7. The reaction fabric diagram of the  $a$  axis of albite replacing labradorite when the  $X$  vibration direction of labradorite is vertical.  $X$ ,  $Y$ , and  $Z$  are  $X$ ,  $Y$ , and  $Z$  of labradorite, and  $a_l$  and  $c_l$  are  $a$  and  $c$  of labradorite. Poles plotted and contour diagram. The five per cent contour encloses five per cent of 200 poles, *i.e.*, 10 poles.

of poles near the  $a$  axis of labradorite ( $a_l$ ). This latter concentration suggests that when labradorite is replaced by albite the zig-zag chains in the former retain their identity, and that aluminium is replaced by silicon with only a small modification of the silicate framework. The general concentration of poles in the 010 plane probably indicates that the albite has a tendency to grow along the 010 cleavage.

#### *The Optics of the Plagioclases*

In determining the position of the  $a$  crystal axis of albite and labradorite with respect to the vibration directions of light through the minerals, an interesting relationship between the indicatrix and the  $a$  crystal axis was noted. Figure 8 shows a lower hemisphere stereographic plot of the  $a$  axes of plagioclase when the  $X$ ,  $Y$  and  $Z$  vibration directions are in the positions shown. The  $a$  axes lie very close to the plane of  $X$  and  $Y$ . Figure 9 shows a lower hemisphere plot of the  $XY$  planes of the plagioclases when the  $a$  crystal axis is vertical (cf. Winchell 1951, Fig. 172, p. 274).



The rotation of the  $XY$  plane about the  $a$  axis in passing from anorthite to albite is worthy of note. Figure 10 is a series of three dimensional diagrams showing how in passing from anorthite to albite there is a clockwise rotation of the  $XY$  plane of the indicatrix about the  $a$  crystal axis with, at the same time, a rotation of  $X$  and  $Y$  in a clockwise direction within the plane.

This is a relatively simple way of visualising the position of the indicatrix in the plagioclase and perhaps indicates that the zig-zag chains in the plagioclase structure, which are parallel to the  $a$  crystal axes, are exerting some controlling influence over the orientation of the indicatrix.

#### THE PREFERRED ORIENTATION OF CRYSTAL STRUCTURES

Preferred orientation of one mineral with respect to another may possibly be brought about by exsolution, simultaneous crystallization, parallel growth, or replacement.

#### Exsolution

Minerals which form solid solutions contain ions of about equal radius and valency, and have similar crystal structures. When exsolution takes

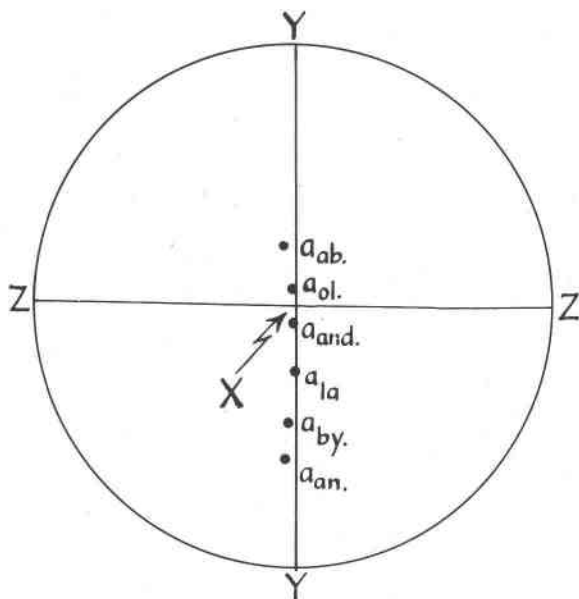


FIG. 8. Optic orientation of the plagioclases. Lower hemisphere, stereographic plot showing the movement of the  $a$  axes of the plagioclases in the  $XY$  plane.  $X$ ,  $Y$ , and  $Z$  are the principal axes of the plagioclase indicatrix.  $a_{ab}$ — $a_{an}$  are the  $a$  axes of the plagioclases.

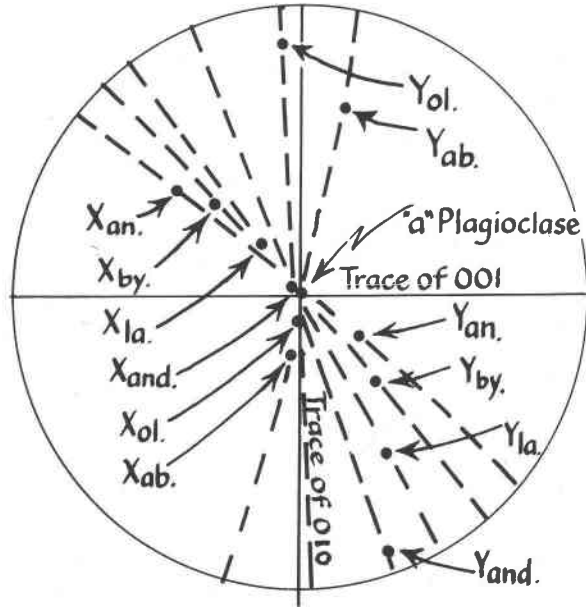


FIG. 9. Optic orientation of the plagioclases. Lower hemisphere stereographic plot showing the rotation of the  $XY$  plane of the plagioclases about the  $a$  crystal axis.  $X_{ab-an}$  and  $Y_{ab-an}$  are the  $X$  and  $Y$  indicatrix axes of the plagioclase.

place the solute and solvent minerals take up relative orientations determined by the structure, *e.g.*, when ilmenite unmixes from magnetite the (0001) planes in the former are parallel to the (111) planes in the latter. Both these planes contain some sheets of oxygen ions which have similar spacing within the sheets (Edwards 1954, p. 76). Again in the perthites the silicate framework is continuous throughout the whole

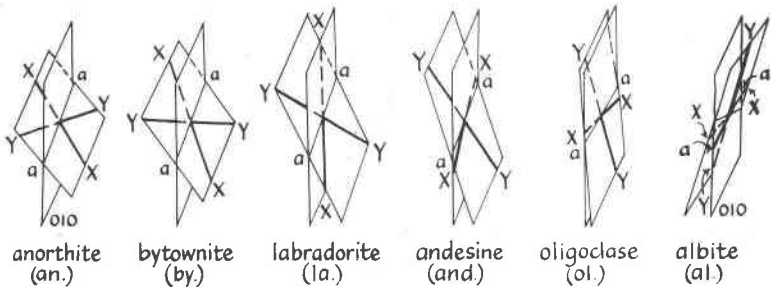


FIG. 10. Optic orientation of the plagioclases. Three dimensional diagram showing the rotation of the  $XY$  plane about the  $a$  axis in the plagioclases.  $X$  and  $Y$  are two principal axes of the plagioclase indicatrix.

crystal, the exsolution involving a redistribution of the  $\text{Na}^+$  and  $\text{K}^+$  ions (Bragg 1937, p. 40).

In both the above cases a reaction fabric diagram of one mineral with respect to the other should give a different but high concentration for each kind of pole.

### *Simultaneous Crystallization*

Simultaneous crystallization usually involves two or more minerals of dissimilar structure. However, it is possible that, in certain cases, crystals may interfere with one another during growth so that one orients the other. Niggli (1954, p. 469) states: "At the outset, because of the Brownian movement, crystal nuclei may impinge on one another and grow by forming aggregates (aggregate growth or initial formation of secondary particles with micellar structure). The mutual orientation of the individual nuclei will be more or less perfect and often only have the character of a twinned intergrowth."

### *Parallel Growth*

In some cases of parallel growth where the minerals have similar crystal structure, relative orientation is obvious from inspection, *e.g.* parallel growth in micas. It is possible also that a reaction fabric may be produced by overgrowth (Niggli 1954, p. 254), and it is apparent from Niggli's figure 150 that the orientation of the hornblende is controlled by the orientation of the augite upon which it has grown (the *c* axes are parallel).

### *Replacement*

Whereas the above three processes are restricted, in general, to igneous rocks and pegmatites, usually as local phenomena, replacement is one of the most common geological processes. Almost all igneous masses show some replacement, whether of metasomatic or autometasomatic origin, and in contact rocks it is almost ubiquitous.

Replacement is generally conceded to be volume for volume, *i.e.*, the amount of a guest required to replace a given host depends on the relative specific gravities. This need not mean a complete destruction of the crystal structure of the mineral being replaced, and in many replacements involving silica and silicates it is probable that associated groups of  $\text{SiO}_4$  tetrahedra from the host are incorporated in the guest mineral. Chemical reactions take the line of least resistance. If a mineral is stable under certain conditions of temperature, pressure, and concentration, then it is formed by that process in which least energy is expended. In the replacement of microcline by quartz for example, it is economical of

energy if  $\text{SiO}_4$  tetrahedra are retained and built into the quartz with a minimum of reorientation, thus producing a reaction fabric.

## REFERENCES

- BRAGG, W. L., 1937. Atomic structure of minerals. Cornell University Press, New York.
- CLARK, R. H., 1956. Petrological study of the Arthur's Seat volcano. Trans. Roy. Soc. Edinburgh, Vol. 63, pp. 37-70.
- EDWARDS, A. B., 1954. Textures of the ore minerals. Australasian Institute of Mining and Metallurgy, Melbourne.
- NIGGLI, P., 1954. Rocks and mineral deposits. W. H. Freeman, San Francisco.
- PHILLIPS, F. C., 1954. The use of stereographic projection in structural geology. Edward Arnold, London.
- WINCHELL, A. N., 1951. Elements of optical mineralogy. Part 2. Wiley, New York.

*Manuscript received November 18, 1960.*